

This is a repository copy of *Change in structure between the $I = 1/2$ states in ^{181}Tl and $^{177,179}\text{Au}$.*

White Rose Research Online URL for this paper:

<https://eprints.whiterose.ac.uk/137334/>

Version: Accepted Version

Article:

Cubiss, J.G. orcid.org/0000-0002-5076-8654, Barzakh, A.E., Andreyev, A.N. orcid.org/0000-0003-2828-0262 et al. (57 more authors) (2018) Change in structure between the $I = 1/2$ states in ^{181}Tl and $^{177,179}\text{Au}$. *Physics Letters B*. pp. 355-363. ISSN 0370-2693

<https://doi.org/10.1016/j.physletb.2018.10.005>

Reuse

This article is distributed under the terms of the Creative Commons Attribution (CC BY) licence. This licence allows you to distribute, remix, tweak, and build upon the work, even commercially, as long as you credit the authors for the original work. More information and the full terms of the licence here:

<https://creativecommons.org/licenses/>

Takedown

If you consider content in White Rose Research Online to be in breach of UK law, please notify us by emailing eprints@whiterose.ac.uk including the URL of the record and the reason for the withdrawal request.

1 Change in structure between the $I = 1/2$ states in ^{181}Tl
2 and $^{177,179}\text{Au}$

3 J. G. Cubiss^{a,b}, A. E. Barzakh^c, A. N. Andreyev^{a,d,b}, M. Al Monthery^a,
4 N. Althubiti^e, B. Andelf^f, S. Antalic^f, D. Atanasov^g, K. Blaum^g,
5 T. E. Cocolios^{h,e,b}, T. Day Goodacre^{b,e}, R. P. de Groote^h, A. de Roubin^g,
6 G. J. Farooq-Smith^{e,h}, D. V. Fedorov^c, V. N. Fedosseev^b, R. Ferrer^h,
7 D. A. Fink^{b,i}, L. P. Gaffney^h, L. Ghys^{h,j}, A. Gredley^k, R. D. Harding^{a,b},
8 F. Herfurth^l, M. Huyse^h, N. Imai^m, D. T. Joss^k, U. Kösterⁿ, S. Kreim^{b,g},
9 V. Liberati^o, D. Lunney^p, K. M. Lynch^{b,e}, V. Manea^{b,p}, B. A. Marsh^b,
10 Y. Martinez Palenzuela^h, P. L. Molkanov^c, P. Mosat^f, D. Neidherr^l,
11 G. G. O'Neill^k, R. D. Page^k, T. J. Procter^{b,e}, E. Rapisarda^{h,b},
12 M. Rosenbusch^q, S. Rothe^{b,r}, K. Sandhu^o, L. Schweikhard^q, M. D. Seliverstov^c,
13 S. Sels^h, P. Spagnoletti^o, V. L. Truesdale^a, C. Van Beveren^h, P. Van Duppen^h,
14 M. Veinhard^b, M. Venhart^s, M. Veselký^s, F. Wearing^k, A. Welker^{b,t},
15 F. Wienholtz^{b,q}, R. N. Wolf^{q,g}, S. G. Zemlyanoy^u, K. Zuber^t

16 ^aDepartment of Physics, University of York, York, YO10 5DD, United Kingdom

17 ^bCERN, CH-1211 Geneva 23, Switzerland

18 ^cPetersburg Nuclear Physics Institute, NRC Kurchatov Institute, 188300 Gatchina, Russia

19 ^dAdvanced Science Research Center (ASRC), Japan Atomic Energy Agency (JAEA),
20 Tokai-mura, Ibaraki 319-1195, Japan

21 ^eSchool of Physics and Astronomy, The University of Manchester, Manchester, M13 9PL,
22 United Kingdom

23 ^fDepartment of Nuclear Physics and Biophysics, Comenius University in Bratislava, 84248
24 Bratislava, Slovakia

25 ^gMax-Planck-Institut für Kernphysik, Saupfercheckweg 1, 69117 Heidelberg, Germany

26 ^hKU Leuven, Instituut voor Kern- en Stralingsfysica, B-3001 Leuven, Belgium

27 ⁱRuprecht-Karls Universität, D-69117 Heidelberg, Germany

28 ^jBelgian Nuclear Research Centre SCK•CEN, Boeretang 200, B-2400 Mol, Belgium

29 ^kOliver Lodge Laboratory, University of Liverpool, Liverpool, L69 7ZE, UK

30 ^lGSI Helmholtzzentrum für Schwerionenforschung GmbH, 64291 Darmstadt, Germany

31 ^mHigh Energy Accelerator Research Organisation (KEK), Oho 1-1, Tsukuba, Ibaraki
32 305-0801, Japan

33 ⁿInstitut Laue Langevin, 6 rue Jules Horowitz, F-38042 Grenoble Cedex 9, France

34 ^oSchool of Engineering and Science, University of the West of Scotland, Paisley PA1 2BE,
35 United Kingdom

36 ^pCSNSM-IN2P3-CNRS, Université Paris-Sud, 91406 Orsay, France

37 ^qErnst-Moritz-Arndt-Universität, Institut für Physik, 17487 Greifswald, Germany

38 ^rInstitut für Physik, Johannes Gutenberg-Universität Mainz, D-55128 Mainz, Germany

39 ^sInstitute of Physics, Slovak Academy of Sciences, 845 11 Bratislava, Slovakia

40 ^tTechnische Universität Dresden, 01069 Dresden, Germany

41 ^uJoint Institute of Nuclear Research, 141980 Dubna, Moscow Region, Russia

Email address: james.cubiss@york.ac.uk (J. G. Cubiss)

42 **Abstract**

43 The first accurate measurements of the α -decay branching ratio and half-life
44 of the $I^\pi = 1/2^+$ ground state in ^{181}Tl have been made, along with the first
45 determination of the magnetic moments and $I = 1/2$ spin assignments of the
46 ground states in $^{177,179}\text{Au}$. The results are discussed within the complementary
47 systematics of the reduced α -decay widths and nuclear g factors of low-lying,
48 $I^\pi = 1/2^+$ states in the neutron-deficient lead region. The findings shed light on
49 the unexpected hindrance of the $1/2^+ \rightarrow 1/2^+$, $^{181}\text{Tl}^g \rightarrow ^{177}\text{Au}^g$ α decay, which
50 is explained by a mixing of $\pi 3s_{1/2}$ and $\pi 2d_{3/2}$ configurations in $^{177}\text{Au}^g$, whilst
51 $^{181}\text{Tl}^g$ remains a near-pure $\pi 3s_{1/2}$. This conclusion is inferred from the g factor
52 of $^{177}\text{Au}^g$ which has an intermediate value between those of $\pi 3s_{1/2}$ and $\pi 2d_{3/2}$
53 states. A similar mixed configuration is proposed for the $I^\pi = 1/2^+$ ground
54 state of ^{179}Au . This mixing may provide evidence for triaxial shapes in the
55 ground states in these nuclei.

56 *Keywords:* nuclear physics, decay spectroscopy, laser spectroscopy, nuclear
57 deformation, gold nuclei, thallium nuclei

58 **1. INTRODUCTION**

59 Low-energy shape coexistence, whereby states of differing shape compete at
60 low-excitation energies within the same nucleus, is an intriguing and complex
61 facet of nuclear structure [1]. This phenomenon results from an interplay be-
62 tween two opposing behaviours: the stabilising effect of shell closures which
63 preserves sphericity, and residual interactions between protons and neutrons
64 that drive deformation [2]. However, the description of such behaviour remains
65 a challenge for contemporary nuclear theory.

66 To simplify the description of this complex phenomenon, theoretical mod-
67 els often invoke axial and reflection symmetries. However, as highlighted in
68 e.g. Ref [3] for germanium isotopes, the use of such restrictions may lead to
69 problems. In particular, coexisting energy minima at different quadrupole de-
70 formations could be connected by a valley of triaxiality, along which the true
71 energy minimum lies. Therefore, special care should be taken when modelling
72 nuclei that inhabit known or expected regions of triaxiality.

73 The neutron-deficient gold ($Z = 79$) isotopes have proved to be fertile ground
74 for the study of shape coexistence and triaxiality [4, 5, 6, 7, 8, 9, 10, 11, 12,
75 13, 14]. The ground-state structures of odd-mass gold isotopes are seen to
76 gradually evolve as the mass reduces down to $A = 187$ ($N = 108$). This is
77 evidenced by their g factors, spins and parities which change from those of
78 near-pure $\pi 2d_{3/2}$ configurations with $I^\pi = 3/2^+$ for the odd- A isotopes with
79 $A \geq 191$, to mixed $\pi 2d_{3/2}/\pi 3s_{1/2}$ states with $I^\pi = 1/2^+$ in $^{187,189}\text{Au}$ [15,
80 4]. However, these nuclei are seen to retain weakly oblate (near spherical)
81 shapes. A more dramatic change in structure is seen below $A = 187$, with a
82 large increase in the mean-squared charge radius indicating a sudden increase
83 in the ground-state deformation [5, 6, 7]. This transition from weakly oblate to

84 strongly prolate shapes makes these nuclei of particular interest for investigating
85 coexisting structures within the region. The large increase in deformation is
86 accompanied by a change in the ground-state configuration to the $5/2^-$ member
87 of the band, based upon the strongly prolate $1/2[541]$ and/or $3/2[532]$ deformed
88 states of a $\pi 1h_{9/2}$ parentage, as was proposed for $^{181,183,185}\text{Au}$ in Refs. [4, 16, 17].
89 The ground states of the neutron-deficient gold isotopes were predicted to stay
90 strongly deformed until $A \approx 177$, where a return to near-spherical shapes was
91 proposed to occur (see Fig. 31 in Ref.[18]). However, results from in-beam and
92 α -decay studies suggest that this region of strong deformation ends earlier, at
93 $A = 179$, where it is proposed that the ground state returns to a $\pi 2d_{3/2}/\pi 3s_{1/2}$
94 configuration [19, 20, 21].

95 Evidence for triaxial shapes has been found in the neighbouring platinum
96 isotopes. In particular, the magnetic moments of the lowest $3/2^-$ states in the
97 odd- A isotopes $^{187-193}\text{Pt}$ were shown in Ref. [22] (see Fig. 6 therein) to have
98 a strong dependence on the triaxial deformation parameter, γ . Gold isotopes,
99 which can be viewed as a proton coupled to a platinum core, may also display
100 such behaviour. Signatures of triaxiality have been seen in the excited states of
101 some gold isotopes (see Refs. [23, 11, 12, 13] and references within). Thus, it
102 may be possible to observe signs of triaxiality in ground-state magnetic moments
103 of gold nuclei, similar to those seen in the neighbouring platinum isotopes.

104 This article reports on a two-pronged experimental study of the ground
105 and isomeric states of thallium and gold isotopes. First, an α -decay study
106 of the $I = 1/2^+$ ground state in ^{181}Tl ($T_{1/2} = 3.2(3)$ s [24]) was performed
107 to investigate the unexpected hindrance to the decay observed in a study by
108 Andreyev *et al.* [25], at the velocity filter SHIP (GSI). In this work, the authors
109 deduced an upper limit for the α -decay branching ratio of $b_\alpha(^{181}\text{Tl}^g) < 10\%$,
110 which resulted in an upper limit for the reduced α -decay width of $\delta_\alpha^2 < 19$ keV.
111 The latter is notably smaller than those of other unhindered $1/2^+ \rightarrow 1/2^+$ α
112 decays in the region, which typically have values of $\delta_\alpha^2 = 45 - 90$ keV. This
113 raises the question as to the possible cause of hindrance in the $^{181}\text{Tl}^g$ α decay.
114 Recent mean-squared charge radii measurements by Barzakh *et al.* [26] show
115 $^{181}\text{Tl}^g$ to be nearly spherical, with a magnetic moment in good agreement with
116 values for the $I = 1/2^+$ states in other odd- A thallium isotopes, which have
117 near-pure $\pi 3s_{1/2}$ configurations. This proves that there is nothing unusual with
118 the underlying structure of $^{181}\text{Tl}^g$. Therefore, the main goals of the present
119 work were to extract a value for b_α and the half-life ($T_{1/2}$) of $^{181}\text{Tl}^g$, in order
120 to confirm or disprove the hindrance observed in Ref. [25].

121 On the other hand, a difference in configurations between $^{181}\text{Tl}^g$ and its
122 α -decay daughter nucleus, $^{177}\text{Au}^g$, could explain this hindrance. Prior to this
123 work, $^{177}\text{Au}^g$ was tentatively assigned a spin of $I^\pi = (1/2^+, 3/2^+)$, based on the
124 in-beam study by Kondev *et al.* [21], with the most likely configuration being
125 either $1/2^+[411](d_{3/2})$ at oblate deformation with some admixture from $\pi 3s_{1/2}$,
126 or a prolate $3/2^+[402](d_{3/2})$ state.

127 Therefore, in-source laser spectroscopy measurements of $^{177}\text{Au}^g$ were per-
128 formed. The present work provides the first unambiguous measurements of the
129 spins and magnetic moments of $^{177,179}\text{Au}^g$. The new results for $^{181}\text{Tl}^g$ and

130 $^{177,179}\text{Au}^g$ will be discussed within the context of the systematics of reduced α -
131 decay widths for $1/2^+ \rightarrow 1/2^+$ α decays and nuclear g factors of $I = 1/2$ states
132 within the region.

133 2. EXPERIMENT

134 Two experimental campaigns were performed for the isotopes $^{181}\text{Tl}^g$ and
135 $^{177,179}\text{Au}^g$. In both cases the experimental method was the same as that em-
136 ployed in the studies of the thallium isotopic chain presented in Refs. [26, 27].
137 Additional details pertinent to the present work are given below. The radioac-
138 tive thallium and gold nuclei were produced at the ISOLDE facility [28, 29],
139 in spallation reactions induced by a 1.4-GeV proton beam, impinging upon a
140 50 g/cm^2 -thick UC_x target. The proton beam was delivered by the CERN PS
141 Booster with an average current of $2.1\ \mu\text{A}$, in a repeated sequence known as a
142 supercycle that typically consisted of 35–40, $2.4\text{-}\mu\text{s}$ long pulses, with a minimum
143 interval of 1.2 s between each pulse.

144 After proton impact the reaction products diffused through the target matrix
145 and effused towards a hot cavity ion source, kept at a temperature of $\approx 2000\text{ }^\circ\text{C}$.
146 Inside the cavity, the thallium or gold atoms were selectively ionised by the
147 ISOLDE Resonance Ionization Laser Ion Source (RILIS) [30, 31]. The ions
148 were then extracted from the cavity using a 30 kV electrostatic potential and
149 separated according to their mass-to-charge ratio by the ISOLDE GPS mass sep-
150 arator. The mass-separated beam was then delivered to either the ISOLTRAP
151 Multi-Reflection Time-of-Flight Mass Spectrometer (MR-ToF MS) [32] or the
152 Windmill decay station [33, 34], for photoion monitoring during RILIS laser-
153 wavelength scans across the hyperfine structure (hfs) of an atomic transition
154 used in the resonance ionization process (see Fig. 1). Details of the scanning
155 procedures can be found in Ref. [35] for the MR-ToF MS, and Refs. [33, 36] for
156 the Windmill system.

157 As well as hfs scanning, the Windmill decay station was used for the de-
158 cay studies of ^{181}Tl . The mass-separated beam entered the Windmill system
159 through the central hole of an annular silicon detector (Si1) and was implanted
160 into one of ten, $20\ \mu\text{g/cm}^2$ -thick carbon foils mounted on a rotatable wheel. A
161 second surface-barrier silicon detector (Si2) was positioned a few mm behind the
162 foil at the implantation site. Together, Si1+Si2 were used to measure the short-
163 lived α activity at the implantation site. After a fixed number of supercycles
164 the wheel of the Windmill was rotated within a 0.8 s time window, moving the
165 irradiated foil to a decay site, between a pair of closely spaced silicon detectors
166 (Si3 and Si4), which were used to measure long-lived decays. The full-width at
167 half maxima of the recorded α -decay peaks were 22–35 keV, within the energy
168 region of interest ($E_\alpha = 5000\text{--}7000\text{ keV}$).

169 The α -decay study of $^{181}\text{Tl}^g$ was part of the experiment described in Ref. [26],
170 in which the change in mean-squared charge radii and nuclear magnetic dipole
171 moments of the thallium isotopic chain were discussed. During this experiment,
172 a two-step resonant ionisation scheme was used to ionise the thallium isotopes.
173 In the case of ^{181}Tl , only beams of the ground state were produced, as the

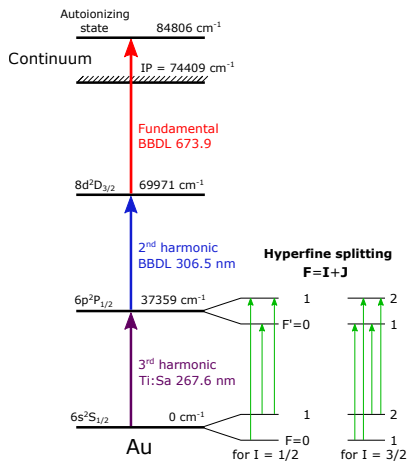


Figure 1: The three-step resonant photoionization scheme used to produce gold ions [37], along with the hyperfine structures (not to scale) expected for a nucleus with spin $I = 1/2$, or $I = 3/2$. The green arrows indicate the allowed transitions between different electronic states: three lines for $I = 1/2$, and four for $I = 3/2$.

174 production rate and half-life of the $I^\pi = 9/2^-$ isomer were too low for its
 175 extraction from the target ($T_{1/2} = 1.40(3)$ ms [19]).

176 In the separate experiment on $^{177,179}\text{Au}^g$, the laser spectroscopy measure-
 177 ments were made using the three-step resonant ionisation scheme shown in
 178 Fig. 1 [37]. The IS and hfs measurements were made upon the 267.7-nm tran-
 179 sition, by scanning a frequency-tripled titanium sapphire (Ti:Sa) laser in a nar-
 180 rowband mode (FWHM bandwidth of 600 MHz before tripling). Two broadband
 181 dye lasers (BBDL; FWHM bandwidth of ≈ 20 GHz) were used for the second
 182 and third excitation steps.

183 3. Results

184 3.1. ^{181}Tl α -decay branching ratio and half-life

185 Figure 2 shows the singles α -decay spectra recorded by the four silicon detec-
 186 tors of the Windmill system, during the α -decay study of $^{181}\text{Tl}^g$. In the spectra,
 187 α decays originating from $^{181}\text{Tl}^g$ and its α -/ β -decay daughter and granddaugh-
 188 ter nuclei (^{181}Hg , ^{181}Au , ^{177}Au and ^{177}Pt) can be seen, along with an uniden-
 189 tified, low-intensity decay at $E_\alpha \approx 5750$ keV in the Si1 and Si2 spectra. Due
 190 to the long half-life of $^{181}\text{Tl}^g$ ($T_{1/2} = 3.2(3)$ s [24]), its α decays are also seen
 191 in Si3 and Si4 after the movement of the Windmill. Energy calibrations for
 192 the silicon detectors were made using the evaluated α -decay energies of ^{181}Hg
 193 ($E_\alpha = 6006(5)$ keV) and ^{177}Pt ($E_\alpha = 5517(4)$ keV) [38], both of which are part
 194 of the ^{181}Tl decay chain and were produced in the same run.

195 It is important to note the proximity in energy of the $^{177}\text{Au}^g$ and $^{181}\text{Tl}^g$ α de-
 196 cays, which differ by just ≈ 20 keV (see Fig. 2 and the following discussion). Be-
 197 cause of this and their relatively long half-lives ($T_{1/2}(^{177}\text{Au}^g) = 1.462(32)$ s [21]),

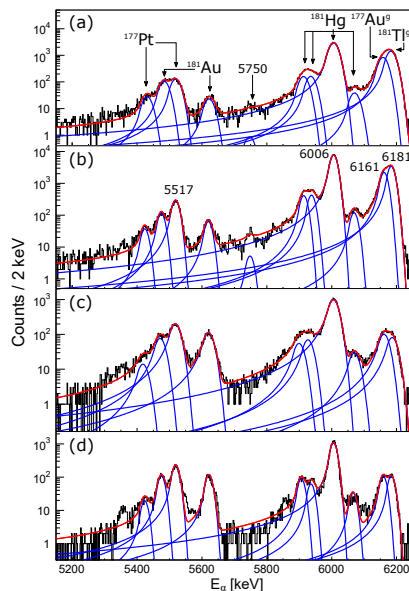


Figure 2: Singles α -decay spectra recorded by (a) Si1, (b) Si2, (c) Si3 and (d) Si4, fitted with crystal ball (CB) functions. The red traces represent the convolution of CB functions fitted to the spectra, the blue traces are the individual components that contribute to the full fit. The peaks belonging to the α decays of ^{177}Pt , ^{181}Au , ^{181}Hg , $^{177}\text{Au}^g$ and $^{181}\text{Tl}^g$ are labelled, along with a weak, unidentified decay present in the Si1 and Si2 spectra, at $E_\alpha \approx 5750$ keV.

198 previous attempts to extract values of b_α and $T_{1/2}$ from the mixed $^{181}\text{Tl}^g + ^{177}\text{Au}^g$
 199 peak have had limited precision [39, 40, 24, 19]. This issue is highlighted in
 200 Fig. 2, in which the energy peaks of the $^{181}\text{Tl}^g$ and $^{177}\text{Au}^g$ α decays are seen
 201 to overlap in all four spectra. This problem could be overcome by using the
 202 α - α correlation method for $^{181}\text{Tl}^g \rightarrow ^{177}\text{Au}^g$ decays at recoil separators, but so
 203 far such studies have resulted in low statistics, making determination of the
 204 branching ratio difficult [40, 24, 19], with only an upper limit of $b_\alpha < 10\%$
 205 reported in Ref. [25].

206 Despite this issue, it was possible to extract an accurate value of $b_\alpha(^{181}\text{Tl}^g)$
 207 in the present work. This was done by fitting the singles α -decay spectra for each
 208 silicon detector separately, the results of which are shown by the red and blue
 209 curves in Fig. 2. The fitting was performed by the ROOT Minuit minimiser [41],
 210 using a binned-likelihood method and Crystal Ball functions [42, 43, 44] to
 211 describe the shape of the α -decay peaks. The parameters of the fits were left
 212 free, but kept such that those defining the tail and the width were the same for
 213 all peaks belonging to the spectrum of each individual detector. The fits yielded
 214 energies of $E_\alpha(^{181}\text{Tl}^g) = 6183(7)$ and $E_\alpha(^{177}\text{Au}^g) = 6159(7)$ keV. These values
 215 are in good agreement with those of Ref. [19]: $E_\alpha(^{181}\text{Tl}^g) = 6181(7)$ keV and
 216 $E_\alpha(^{177}\text{Au}^g) = 6161(7)$ keV, as well as Ref. [21] ($E_\alpha(^{177}\text{Au}^g) = 6160$ keV), where
 217 the isotope $^{177}\text{Au}^g$ was directly produced, and therefore the determination of

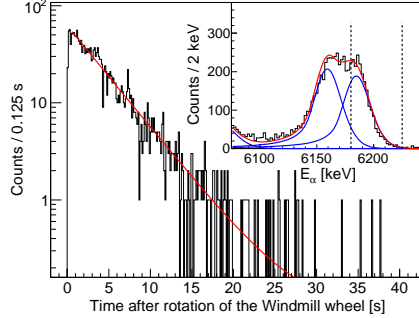


Figure 3: Time distribution of $6180 \leq E_\alpha \leq 6225$ -keV α decays, measured in Si3 and Si4, fitted with an exponential plus constant background function (red curve). The inset shows the sum of the singles- α decay spectra for Si3 and Si4, the blue and red curves are the sum of the fits shown in Figs. 2(c) and (d). The vertical, dashed lines indicate the gating conditions used to produce the decay curve shown in the main panel.

218 E_α had no interference from the presence of $^{181}\text{Tl}^g$.

219 The α -decay branching ratio of $^{181}\text{Tl}^g$ was determined by comparing the
 220 number of detected $^{181}\text{Tl}^g$ and ^{181}Hg α decays taken from the fits, corrected by
 221 the α -decay branching ratio of ^{181}Hg , such that

$$\begin{aligned}
 b_\alpha(^{181}\text{Tl}^g) &= \frac{100\% \times N_\alpha(^{181}\text{Tl}^g)}{N_\alpha(^{181}\text{Tl}^g) + N_\beta(^{181}\text{Tl}^g)} \\
 &= \frac{100\% \times N_\alpha(^{181}\text{Tl}^g)}{N_\alpha(^{181}\text{Tl}^g) + \frac{N_\alpha(^{181}\text{Hg})}{b_\alpha(^{181}\text{Hg})}},
 \end{aligned}
 \tag{1}$$

222 where $N_\alpha(X)$ represents the sum of the counts from all four silicon detectors,
 223 for a particular isotope. Using the evaluated value $b_\alpha(^{181}\text{Hg}) = 27(2)\%$ [38],
 224 an α -decay branching ratio of $b_\alpha(^{181}\text{Tl}^g) = 8.6(6)\%$ was deduced, which is in
 225 agreement with the upper limit of $b_\alpha(^{181}\text{Tl}^g) \leq 10\%$ determined by Andreyev
 226 *et al.* [25].

227 A value of $T_{1/2}(^{181}\text{Tl}^g)$ was extracted from the combined decay curve recorded
 228 in Si3+Si4 (see Fig. 3). By selecting events belonging to the high-energy side
 229 of the combined $^{177}\text{Au}^g + ^{181}\text{Tl}^g$ peak ($6180 \leq E_\alpha \leq 6225$ keV, see Fig. 3 inset),
 230 the contribution of $^{177}\text{Au}^g$ α decays was $< 10\%$ of the total statistics. The
 231 extracted data were fitted with an exponential plus constant background, and a
 232 value of $T_{1/2}(^{181}\text{Tl}^g) = 2.9(1)$ s was extracted. This new value is in agreement
 233 with the literature value of $T_{1/2}(^{181}\text{Tl}^g) = 3.2(3)$ s [24] but is three times more
 234 precise.

235 The E_α , $T_{1/2}$ and b_α values extracted from the present data are compared
 236 with those from previous studies in Table 1. Using results from the current work
 237 and assuming $\Delta L = 0$ (see Sec. 3.2.1 for spin assignment of $^{177}\text{Au}^g$), a value of
 238 $\delta_\alpha^2(^{181}\text{Tl}^g) = 17.9(18)$ keV was deduced using the Rasmussen approach [45].

Table 1: Comparison of the E_α , $T_{1/2}$ and b_α values for the α decays of the ground states of ^{181}Tl and ^{177}Au extracted from the present work and previous studies.

Isotope	E_α [keV]	$T_{1/2}$ [s]	b_α [%]	δ_α^2 [keV]	Reference
$^{181}\text{Tl}^g$	6183(7)	2.9(1)	8.6(6)	17.9(18)	Present work
$^{181}\text{Tl}^g$	6181(7)	—	<10	<19 ¹	[19]
$^{181}\text{Tl}^g$	6186(10)	3.2(3)	—	—	[24]

239 *3.2. Ground-state spins and magnetic dipole moments of $^{177,179}\text{Au}^g$*

240 *3.2.1. Spins of $^{177,179}\text{Au}^g$*

241 Although ^{177}Au has two long-lived states ($T_{1/2} = 1462(32)$ ms and $E_\alpha =$
 242 6161(7) keV for the ground state, and $T_{1/2} = 1180(12)$ ms and $E_\alpha = 6124(7)$ keV
 243 for the isomeric state [21, 19]), their respective hfs of the 267.6-nm transition do
 244 not overlap. Thus, with the laser tuned to the correct frequency, it is possible to
 245 obtain a clean $^{177}\text{Au}^g$ singles α -decay spectrum (see inset of Fig. 4(a), in which
 246 only the 6161-keV α decay of $^{177}\text{Au}^g$ is present). By gating on this peak, it was
 247 possible to extract a pure $^{177}\text{Au}^g$ hfs spectrum (Fig. 4(a)) from which a value
 248 of μ was deduced².

249 The hfs spectrum for $^{177}\text{Au}^g$, an example of which is shown in the main panel
 250 of Fig. 4(a), represents the measured α -decay rate as a function of the scanned
 251 laser frequency. The positions of the hyperfine components as a function of the
 252 scanning laser frequency are determined by the formula:

$$\nu^{F,F'} = \nu_0 + a(6p) \cdot \frac{K'}{2} - a(6s) \cdot \frac{K}{2}, \quad (2)$$

253 where ν_0 is the centroid frequency of the hfs, the prime symbol denotes the upper
 254 level of the atomic transition (see Fig. 1), $K = F(F+1) - I(I+1) - J(J+1)$, F is
 255 the quantum number for the total angular momentum of the atomic level, I and
 256 J are the quantum numbers for the nuclear spin and the angular momentum for
 257 the electronic state, respectively, and $a(nl)$ is the magnetic hyperfine coupling
 258 constant for the atomic level with the quantum numbers n and l .

259 As the upper and lower levels of the scanned transition both have $J = 1/2$, it
 260 is possible to distinguish between the two possibilities of nuclear spin, $I = 1/2$
 261 and $I = 3/2$, by the number of peaks present in the hfs spectra shown in
 262 Fig. 4. For $I = 1/2$, the $F = 0 \rightarrow F' = 0$ excitation is forbidden. Therefore
 263 only three transitions are possible (see Fig. 1), with a hfs peak intensity profile
 264 of 1:2:1. In the case of $I = 3/2$, four peaks with a 5:5:1:5 relative intensity
 265 ratio would be expected (the blue arrows in Fig. 4 approximate the expected

²The results for the isomeric state will be published elsewhere [46]. They confirm that the hfs of $^{177}\text{Au}^g$ and $^{177}\text{Au}^m$ do not overlap.

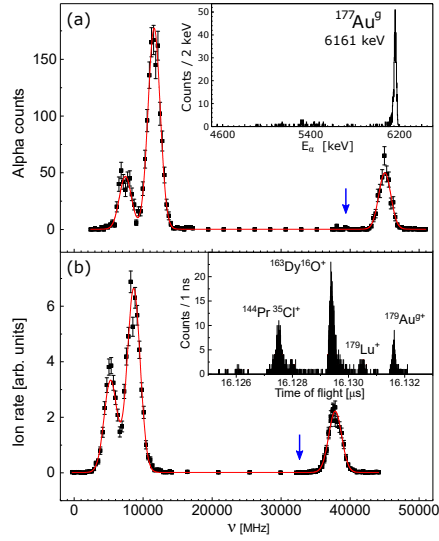


Figure 4: The hfs spectra for (a) $^{177}\text{Au}^g$ (Windmill) and (b) $^{179}\text{Au}^g$ (MR-ToF MS). The insets in panels (a) and (b) show the singles α -decay and the time-of-flight spectra recorded during the laser scans for $^{177}\text{Au}^g$ and $^{179}\text{Au}^g$, measured by the Windmill and MR-ToF MS, respectively. Along with the ^{179}Au nuclei of interest, a number of mass contaminants can be seen in the $A = 179$ time-of-flight spectrum. In order to produce the hfs spectrum of $^{179}\text{Au}^g$ shown in panel (b), a ToF gate was placed upon its peak shown in the inset. The zero frequency corresponds to the hfs centroid of stable $^{197}\text{Au}^g$. Both hfs spectra contain only three peaks, which firmly establishes that $^{177,179}\text{Au}^g$ have $I = 1/2$. The blue arrows indicate the approximate location a fourth peak would be expected, were $I(^{177,179}\text{Au}^g) = 3/2$ (see text for details).

266 position of the lowest-intensity peak in the case of $I = 3/2$). Thus, the three
 267 components of the hfs spectrum in Fig. 4(a) and the observed intensity ratios
 268 (similar to the expected 1:2:1 profile) unambiguously prove $I(^{177}\text{Au}^g) = 1/2$
 269 (which justifies the use of $\Delta L = 0$ in the Rasmussen calculations of Sec. 3.1, for
 270 $I^\pi = 1/2^+ \text{ } ^{181}\text{Tl}^g$ [26]). The same situation is seen for $^{179}\text{Au}^g$, the hfs of which
 271 also possesses three peaks and an intensity profile that prove it too has $I = 1/2$
 272 (see Fig. 4(b)).

273 In passing we note that this new spin assignment for $^{179}\text{Au}^g$, combined with
 274 the unhindered nature of its $E_\alpha = 5848(5)$ keV [38] α decay (see Fig. 5(a)),
 275 establishes a spin and parity of $I^\pi = 1/2^+$ for the state in the daughter nucleus
 276 ^{175}Ir that is fed by this α decay. Interestingly, previous in-beam studies did not
 277 find such a state and suggested that the ^{175}Ir ground state is $I^\pi = 5/2^-$ [47, 48].
 278 The structure of the low-lying states in ^{175}Ir will be further investigated in a
 279 forthcoming, dedicated decay study [49].

280 3.2.2. Magnetic dipole moments of $^{177,179}\text{Au}^g$

281 The extracted hfs spectra were fitted using Voigt profiles [26], with $I = 1/2$,
 282 resulting in values of $a(6s, ^{177}\text{Au}^g) = 66940(260)$ MHz and $a(6s, ^{179}\text{Au}^g) =$
 283 $58460(230)$ MHz.

284 To determine the magnetic moments, the prescription of Ekström *et al.* was
 285 used [4]:

$$\mu = \frac{a(6s)I}{29005} \pm 0.012, \quad \text{for } I = j = l \pm \frac{1}{2}. \quad (3)$$

286 This relationship takes into account the hyperfine anomaly [50], by applica-
 287 tion of the Moskowitz-Lombardi empirical rule [51]. This rule holds for single-
 288 particle shell model states with an orbital angular momentum, l , and a total
 289 angular momentum, j . However, in a recent work by Frömmgen *et al.* [52], it
 290 was shown that the Moskowitz-Lombardi rule could not be applied to $I^\pi = 1/2^+$
 291 states in cadmium isotopes. Analysis of the hyperfine anomaly for thallium iso-
 292 topes with an odd proton in a $\pi 3s_{1/2}$ orbital shows that the correction factor
 293 of ± 0.012 in Eq. 3 should be replaced by a value of 0.05 [53]. The long-lived
 294 $I^\pi = 1/2^+$ states in gold isotopes can be an admixture of $\pi 3s_{1/2}(j = l + 1/2)$,
 295 and $\pi 2d_{3/2}(j = l - 1/2)$ states (see below). Therefore, a simplified version of
 296 Eq. (3) was used³, where the correction factor was removed and the uncertainty
 297 on μ was increased by 0.05, accordingly. This yields $\mu(^{177}\text{Au}^g) = 1.15(5) \mu_N$
 298 and $\mu(^{179}\text{Au}^g) = 1.01(5) \mu_N$.

299 4. DISCUSSION

300 Figure 5(a) shows the δ_α^2 values for $1/2^+ \rightarrow 1/2^+$ α decays, calculated using
 301 the Rasmussen approach [45], for gold ($Z = 79$, pink downwards triangles) [54,
 302 55, 56, 46], astatine ($Z = 85$, red circles) [57, 58, 59, 60, 61], bismuth ($Z = 83$,

³This is the same approach as used in Refs. [5, 6, 7, 8, 10]

303 blue squares) [62, 57, 58, 38, 63], thallium ($Z = 81$, black triangles) [54, 56] and
 304 iridium isotopes ($Z = 77$, teal crosses) [64, 55, 56, 65]. The reader is reminded
 305 that unhindered α decays for odd- A nuclei within this region have typical values
 306 of $\delta_\alpha^2 = 45 - 90$ keV (indicated by the green, shaded region in Fig. 5(a)). In
 307 general terms, the δ_α^2 values decrease as $N \rightarrow 126$, due to a lowering of the
 308 α -particle preformation probability (see Refs. [66, 67] for details). One sees this
 309 effect in the astatine and bismuth isotopes (as well as in the even- Z polonium,
 310 radon, radium and thorium isotopes, not shown in the plot). However, ^{181}Tl
 311 ($N = 100$) is far from the $N = 126$ shell closure and so this effect is not pertinent
 312 to the following discussion.

313 The value of $\delta_\alpha^2(^{181}\text{Tl}^g; 1/2 \rightarrow 1/2) = 17.9(18)$ keV deduced in the present
 314 work is smaller than typical $\delta_\alpha^2(1/2 \rightarrow 1/2)$ values in the region, in particular,
 315 those belonging to $^{177,179}\text{Tl}$ ($\delta_\alpha^2 = 56(19)$ and $50(3)$ keV, respectively) which
 316 are in good agreement with the observed systematics. A comparison of the δ_α^2
 317 value of $^{181}\text{Tl}^g$ and the unhindered α decay of its even-even neighbour, $^{180}\text{Hg}^4$,
 318 yields a hindrance factor of $\text{HF}_\alpha = 4.1(5)$, indicating that the $^{181}\text{Tl}^g$ α decay
 319 is hindered. The mean-squared charge radii and magnetic moment results from
 320 Ref. [26] showed $^{181}\text{Tl}^g$ to be spherical, with a near-pure $\pi 3s_{1/2}$ configuration.
 321 These results are supported by potential energy surface (PES) calculations,
 322 made using the finite-range liquid drop model (FRDM) for the macroscopic part
 323 of the energy functional [71]. The results of these calculations for ^{181}Tl have
 324 a lowest-energy minimum that corresponds to a spherical nucleus (see Fig. 6).
 325 Thus, both the experimental results and the theoretical calculations show that
 326 there is nothing unusual with the structure of $^{181}\text{Tl}^g$. Therefore, the observed
 327 hindrance in the $^{181}\text{Tl}^g$ α decay must be due to an unusual configuration in the
 328 daughter nucleus, $^{177}\text{Au}^g$.

329 This configuration may be probed by investigating the g factor of $^{177}\text{Au}^g$.
 330 In Fig. 5(b), the g factors for the $I = 1/2$ ground/isomeric states are plotted
 331 for gold (pink, downwards triangles [72] and references therein), astatine (red
 332 circles) [35], bismuth (blue squares) [77] and thallium (black triangles) [73, 74,
 333 75, 76, 26] isotopes, along with those of the $I = 3/2$ ground states in gold nuclei
 334 (green diamonds) [72]. It is worth noting the remarkable constancy of the g
 335 factors as a function of neutron number for the thallium, bismuth and astatine
 336 isotopes. The data plotted in Fig. 5(b) show that the g factor for $^{181}\text{Tl}^g$ is
 337 in good agreement with those of other $I = 1/2$, odd- A thallium isotopes, as
 338 well as those of the astatine and bismuth chain. These nuclides, with $g \approx 3.2$,
 339 are characteristic of nuclei with a valence proton occupying a predominantly
 340 $\pi 3s_{1/2}$ orbital. In passing, we also note that the $I = 1/2$ states in the astatine
 341 and bismuth nuclei belong to weakly-deformed intruder configurations [77, 35],
 342 whereas in thallium nuclei they are the normal, spherical states [26]. Thus,
 343 at least for small deformations, $g(\pi 3s_{1/2})$ is not sensitive to variations in the
 344 quadrupole deformation parameter, ϵ_2 (see also Ref. [78]).

⁴A value of $\delta_\alpha^2(^{180}\text{Hg}) = 74(4)$ keV was deduced for the unhindered ^{180}Hg decay, using
 data taken from Refs. [68, 69, 70]

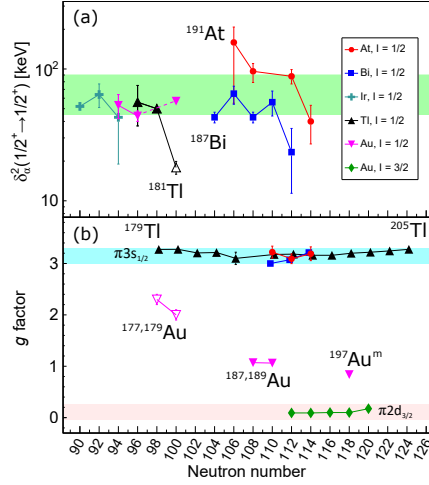


Figure 5: (a) The reduced widths for $I = 1/2 \rightarrow 1/2$ α decays, the green shaded region represents $\delta_\alpha^2 = 45 - 90$ keV, typical of unhindered decays in odd- A isotopes in the region; (b) nuclear g factors, for $I = 1/2$ ground and isomeric states of isotopes surrounding the $Z = 82$ shell closure, along with the $I = 1/2$ (pink, downwards triangles) and $I = 3/2$ (green diamonds) states in gold isotopes, the blue and pink shaded regions represent the approximate g -factor values for near-pure $\pi 3s_{1/2}$ and $\pi 2d_{3/2}$ states, respectively. The hollow symbols for $\delta_\alpha^2(^{181}\text{Tl}^g)$ and $g(^{177,179}\text{Au}^g)$ are the results of the present work.

345 In contrast to those of the near-pure $\pi 3s_{1/2}$ configurations in the thallium,
 346 bismuth and astatine isotopes, $g(^{177}\text{Au}^g)$ is noticeably smaller. This suggests
 347 that $^{177}\text{Au}^g$ has a different structure.

348 To understand this fact, we first note that the $I = 3/2$ states in $^{191-199}\text{Au}$
 349 with $g \approx 0.1$ are dominated by a $\pi 2d_{3/2}$ configuration. All five measured g
 350 factors for the $I = 1/2$ states in $^{177,179,187,189,197}\text{Au}$ lie between the values of the
 351 $g(\pi 3s_{1/2})$ and $g(\pi 2d_{3/2})$ (see Fig. 5(b)). This indicates that these states have
 352 mixed $\pi 3s_{1/2}/\pi 2d_{3/2}$ configurations. The values of $g(^{187,189,197}\text{Au}; I = 1/2)$ are
 353 closer to those of the $I = 3/2$ states in heavier gold isotopes, which suggests
 354 their configurations are primarily $\pi 2d_{3/2}$. In contrast to this, the values of
 355 $g(^{177,179}\text{Au}^g)$ from the present work lie closer to those of $g(\pi 3s_{1/2})$, and appear
 356 to approach the latter with decreasing neutron number. This shift reveals a
 357 change in the dominant component of the wavefunction and a trend towards
 358 near-pure $\pi 3s_{1/2}$ configurations in the lightest gold isotopes. Furthermore, the
 359 hindrance in the $^{181}\text{Tl}^g \rightarrow ^{177}\text{Au}^g$ α decay could be accounted for by a mixed
 360 $\pi 3s_{1/2}/\pi 2d_{3/2}$ configuration in $^{177}\text{Au}^g$ daughter nucleus, in comparison to the
 361 near-pure $\pi 3s_{1/2}$ configuration in $^{181}\text{Tl}^g$.

362 In order to better understand the structures of $^{177,179}\text{Au}^g$ it is instructive
 363 to explore the nature of the $I = 1/2$ states in $^{187,189}\text{Au}$ in more detail. The
 364 first measurement of $g(^{187}\text{Au}^g; I = 1/2) = 1.44(14)$ ($\mu = 0.72(7) \mu_N$) was made
 365 by Ekström *et al.* [4]. Particle-plus-Triaxial Rotor Model (PTRM) calculations
 366 showed that $g(^{187}\text{Au}^g; I = 1/2)$ has a high sensitivity to the degree of axial

367 asymmetry, γ (see Fig. 7 in Ref. [4]). Using these calculations, the authors
368 proposed that $^{187}\text{Au}^g$ was triaxial.

369 However, subsequent measurements performed by Wallmeroth *et al.* [7] (con-
370 firmed by Savard [8]) found $g(^{187}\text{Au}^g; I = 1/2) = 1.07(3)$ (shown in Fig. 5).
371 Using the results from the PTRM calculations in Ref. [4], this new value was
372 explained by a weak, oblate deformation, with no triaxiality (see discussion in
373 Ref. [7]).

374 Further PTRM calculations were performed for $^{187,189}\text{Au}$, by Passler *et*
375 *al.* [9], using combinations of quadrupole, hexadecapole and triaxial degrees
376 of freedom, and modified oscillator or Woods-Saxon single-particle potentials.
377 Again, the calculated g factors of $I = 1/2$ states were seen to be highly sensi-
378 tive to variations in γ . The results of the calculations showed that the g
379 factors of the $I = 1/2$ states in $^{187,189}\text{Au}$ were best described by weakly-
380 oblate, axially-symmetric deformations, with some hexadecapole contribution,
381 and mixed $\pi 3s_{1/2}/\pi 2d_{3/2}$ configurations.

382 In contrast to the PTRM results, the lowest-energy minima in the PES
383 calculations for $^{187,189}\text{Au}$ are triaxial (see Fig. 6), albeit γ soft [71]. However, in
384 the PES of ^{187}Au , there is another minimum at $\gamma \approx 55^\circ$, $\epsilon_2 \approx 0.15$. This may
385 correspond to the weakly-deformed, axially-symmetric oblate states proposed
386 by Wallmeroth and Passler [7, 9].

387 If one applies the same PTRM considerations used for $^{187,189}\text{Au}^g$ to $^{177,179}\text{Au}^g$,
388 the results from the present work are best described by assuming $|\epsilon_2| \approx 0.18$
389 and $25^\circ < \gamma < 30^\circ$. Similar conclusions may be drawn from the PES plotted
390 in Fig. 6, in which the lowest-energy minima for $^{177,179}\text{Au}$ correspond to nuclei
391 with $|\epsilon_2| \approx 0.15$, $\gamma \approx 30^\circ$.

392 To summarise, the degree of mixing between $\pi 3s_{1/2}$ and $\pi 2d_{3/2}$ shell-model
393 orbitals is crucial when describing the $I = 1/2$ states in the odd- A gold nu-
394 clei, with $A \leq 179$. Two completely different phenomena, reduced α -decay
395 widths and magnetic dipole moments, point towards such mixed structures in
396 $^{177,179}\text{Au}^g$. This may also be an indication of triaxiality in these nuclei, how-
397 ever, a more rigorous theoretical interpretation is required. The use of beyond
398 mean-field techniques may clarify the role of mixing between configurations of
399 different deformations in cases with γ -soft minima in the PES, such as those of
400 the present work.

401 5. CONCLUSION

402 In this study, the b_α and $T_{1/2}$ values of $^{181}\text{Tl}^g$ have been determined, along
403 with spins and magnetic dipole moments of $^{177,179}\text{Au}^g$. The results prove that
404 the α decay of $^{181}\text{Tl}^g$ is hindered, which is surprising for a decay between states
405 of equal spin. The reason for this hindrance is evident from the measured g
406 factor of $^{177}\text{Au}^g$, which lies between those of states dominated by a $\pi 3s_{1/2}$ or
407 $\pi 2d_{3/2}$ orbital, indicating that $^{177}\text{Au}^g$ has a mixed $\pi 3s_{1/2}/\pi 2d_{3/2}$ configuration.
408 Based on the similarity in their g factors, the $I = 1/2$ ground state of ^{179}Au is
409 proposed to have a similar, mixed configuration to that of $^{177}\text{Au}^g$.

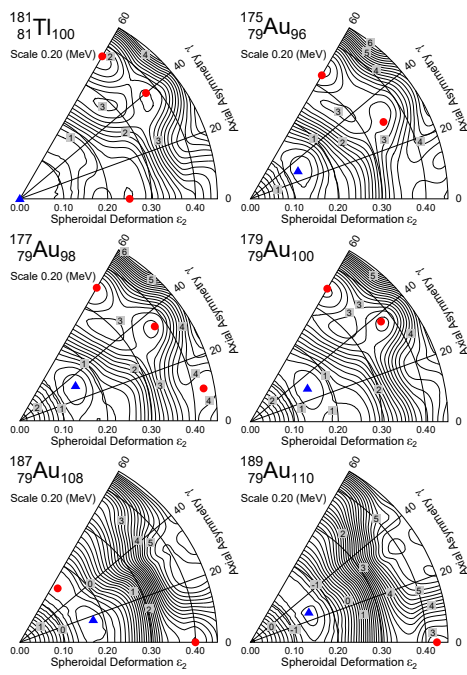


Figure 6: Potential energy surface calculations for ^{181}Tl and $^{175,177,179,187,189}\text{Au}$ [71]. The blue triangles indicate the lowest-energy minimum, and the red spots other minima in the potential energy surfaces.

410 The presence of mixed $\pi 3s_{1/2}/\pi 2d_{3/2}$ states could be a possible indication of
 411 triaxiality in the very neutron-deficient gold nuclei. However, further theoretical
 412 investigations are required to understand the relationship between these two
 413 phenomena. The highlighted interplay between mixing, triaxiality and shape
 414 coexistence is an important guide for constraining PES calculations that will
 415 accompany the next experimental step for g factor measurements for $N < 98$.
 416 Extending the measurements of magnetic dipole moments for $I = 1/2$ states
 417 in the gold nuclei further towards the proton drip line will help to elucidate
 418 whether they have mixed $\pi 3s_{1/2}/\pi 2d_{3/2}$ configurations, as in $^{177,179}\text{Au}^g$, or if
 419 their structures evolve to near-pure $\pi 3s_{1/2}$ states. Indeed, results from α - and
 420 proton-decay studies of $^{171,173}\text{Au}$ suggest that they possess spherical, $I^\pi = 1/2^+$
 421 ground states [54, 79, 80].

422 For example, the δ_α^2 value of the $I^\pi = 1/2^+$ state in ^{179}Tl matches well with
 423 those of other unhindered α decays (see Fig. 5), suggesting that $^{175}\text{Au}^g$ has a
 424 near-pure $\pi 3s_{1/2}$ configuration. However, the PES plot of ^{175}Au shown in Fig. 6
 425 would suggest that the ground state of ^{175}Au is triaxial, and may have a similar
 426 structure to $^{177,179}\text{Au}^g$. Thus, laser spectroscopy measurements of the $I = (1/2)$
 427 state in ^{175}Au ($T_{1/2} = 207(7)$ ms [56]) are essential in gaining a better under-
 428 standing of the evolving structures within the region. Such measurements are
 429 expected to be within the capabilities of current radioactive ion beam facilities.

430 ACKNOWLEDGEMENTS

431 We thank A. Pastore and P. Becker for their helpful discussions and would
 432 like to acknowledge the support of the ISOLDE Collaboration and technical
 433 teams. This work was done with support from the European Union’s Horizon
 434 2020 Framework research and innovation programme under grant agreement
 435 no. 654002 (ENSAR2), by grants from the U.K. Science and Technology Fa-
 436 cilities Council, by FWO-Vlaanderen (Belgium), by GOA/2010/010 (BOF KU
 437 Leuven), by the Interuniversity Attraction Poles Programme initiated by the
 438 Belgian Science Policy Office (BriX network P7/12), by the Slovak Research
 439 and Development Agency (Contract No. APVV-14-0524) and the Slovak Grant
 440 Agency VEGA (Contract No. 1/0532/17), by the Slovak Research and Develop-
 441 ment Agency under Contract No. APVV-15-0225, and the Slovak Grant Agency
 442 VEGA (Contract No. 2/0129/17), and for the received funding through the Eu-
 443 ropean Union’s Seventh Framework Programme for Research and Technological
 444 Development under Grant Agreements 262010 (ENSAR), 267194 (COFUND),
 445 and 289191 (LA3NET).

446 References

- 447 [1] Editors: J. L. Wood and K. Heyde, A focus on shape coexistence in nuclei,
 448 A focus on shape coexistence in nuclei, Journal of Physics G: Nuclear and
 449 Particle Physics 43.

- 450 [2] K. Heyde, J. L. Wood, Shape coexistence in atomic nuclei, *Reviews of*
451 *Modern Physics* 83 (4) (2011) 1467–1521. doi:[10.1103/RevModPhys.83.](https://doi.org/10.1103/RevModPhys.83.1467)
452 [1467](https://doi.org/10.1103/RevModPhys.83.1467).
- 453 [3] L. Guo, J. A. Maruhn, P.-G. Reinhard, Triaxiality and shape coexistence
454 in germanium isotopes, *Physical Review C* 76 (3) (2007) 034317. doi:
455 [10.1103/PhysRevC.76.034317](https://doi.org/10.1103/PhysRevC.76.034317).
- 456 [4] C. Ekström, L. Robertsson, S. Ingelman, G. Wannberg, I. Ragnarsson,
457 Nuclear ground-state spin of ^{185}Au and magnetic moments of 187 , ^{188}Au ,
458 *Nuclear Physics A* 348 (1) (1980) 25–44. doi:[10.1016/0375-9474\(80\)](https://doi.org/10.1016/0375-9474(80)90543-6)
459 [90543-6](https://doi.org/10.1016/0375-9474(80)90543-6).
- 460 [5] K. Wallmeroth, G. Bollen, A. Dohn, P. Egelhof, J. Grüner, F. Lindenlauf,
461 U. Krönert, J. Campos, A. Rodriguez Yunta, M. J. G. Borge, A. Venu-
462 gopalan, J. L. Wood, R. B. Moore, H. J. Kluge, Sudden change in the
463 nuclear charge distribution of very light gold isotopes, *Physical Review*
464 *Letters* 58 (15) (1987) 1516–1519. doi:[10.1103/PhysRevLett.58.1516](https://doi.org/10.1103/PhysRevLett.58.1516).
- 465 [6] U. Krönert, S. Becker, G. Bollen, M. Gerber, T. Hilberath, H. J. Kluge,
466 G. Passler, Observation of strongly deformed ground-state configurations
467 in ^{184}Au and ^{183}Au by laser spectroscopy, *Zeitschrift für Physik A Atomic*
468 *Nuclei* 331 (4) (1988) 521–522. doi:[10.1007/BF01291911](https://doi.org/10.1007/BF01291911).
- 469 [7] K. Wallmeroth, G. Bollen, A. Dohn, P. Egelhof, U. Krönert, M. J. G. Borge,
470 J. Campos, A. Rodriguez Yunta, K. Heyde, C. De Coster, J. L. Wood, H.-J.
471 Kluge, Nuclear shape transition in light gold isotopes, *Nuclear Physics A*
472 493 (2) (1989) 224–252. doi:[10.1016/0375-9474\(89\)90396-5](https://doi.org/10.1016/0375-9474(89)90396-5).
- 473 [8] G. Savard, J. E. Crawford, J. K. P. Lee, G. Thekkadath, H. T. Duong,
474 J. Pinard, F. Le Blanc, P. Kilcher, J. Obert, J. Oms, J. C. Putaux,
475 B. Roussiere, J. Sauvage, Laser spectroscopy of laser-desorbed gold
476 isotopes, *Nuclear Physics A* 512 (2) (1990) 241–252. doi:[10.1016/](https://doi.org/10.1016/0375-9474(90)93192-9)
477 [0375-9474\(90\)93192-9](https://doi.org/10.1016/0375-9474(90)93192-9).
- 478 [9] G. Passler, J. Rikavska, E. Arnold, H.-J. Kluge, L. Monz, R. Neugart,
479 H. Ravn, K. Wendt, Quadrupole moments and nuclear shapes of neutron-
480 deficient gold isotopes, *Nuclear Physics A* 580 (2) (1994) 173–212. doi:
481 [10.1016/0375-9474\(94\)90769-2](https://doi.org/10.1016/0375-9474(94)90769-2).
- 482 [10] F. Le Blanc, J. Obert, J. Oms, J. C. Putaux, B. Roussière, J. Sauvage,
483 J. Pinard, L. Cabaret, H. T. Duong, G. Huber, M. Krieg, V. Sebastian,
484 J. Crawford, J. K. P. Lee, J. Genevey, F. Ibrahim, Nuclear Moments and
485 Deformation Change in ^{184}Au , from Laser Spectroscopy, *Physical Re-*
486 *view Letters* 79 (12) (1997) 2213–2216. doi:[10.1103/PhysRevLett.79.](https://doi.org/10.1103/PhysRevLett.79.2213)
487 [2213](https://doi.org/10.1103/PhysRevLett.79.2213).
- 488 [11] S. C. Wang, X. H. Zhou, Y. D. Fang, Y. H. Zhang, N. T. Zhang, B. S.
489 Gao, M. L. Liu, J. G. Wang, F. Ma, Y. X. Guo, S. C. Li, X. L. Yan, L. He,

- 490 Z. G. Wang, F. Fang, X. G. Wu, C. Y. He, Y. Zheng, Z. M. Wang, G. X.
491 Dong, F. R. Xu, Level structure in the transitional nucleus ^{195}Au , *Physical*
492 *Review C* 85 (2) (2012) 027301. doi:10.1103/PhysRevC.85.027301.
- 493 [12] G. D. Dracoulis, G. J. Lane, H. Watanabe, R. O. Hughes, N. Palalani, F. G.
494 Kondev, M. P. Carpenter, R. V. F. Janssens, T. Lauritsen, C. J. Lister,
495 D. Seweryniak, S. Zhu, P. Chowdhury, W. Y. Liang, Y. Shi, F. R. Xu,
496 Three-quasiparticle isomers and possible deformation in the transitional
497 nuclide, ^{195}Au , *Physical Review C* 87 (1) (2013) 014326. doi:10.1103/
498 *PhysRevC.87.014326*.
- 499 [13] M. Venhart, F. A. Ali, W. Ryssens, J. L. Wood, D. T. Joss, A. N. An-
500 dreyev, K. Auranen, B. Bally, M. Balogh, M. Bender, R. J. Carroll, J. L.
501 Easton, P. T. Greenlees, T. Grahn, P.-H. Heenen, A. Herzán, U. Jakobsson,
502 R. Julin, S. Juutinen, D. Klč, J. Konki, E. Lawrie, M. Leino, V. Matoušek,
503 C. G. McPeake, D. O'Donnell, R. D. Page, J. Pakarinen, J. Partanen,
504 P. Peura, P. Rahkila, P. Ruotsalainen, M. Sandzelius, J. Sarén, B. Saygi,
505 M. Sedlák, C. Scholey, J. Sorri, S. Stolze, A. Thornthwaite, J. Uusitalo,
506 M. Veselský, De-excitation of the strongly coupled band in ^{177}Au and im-
507 plications for core intruder configurations in the light Hg isotopes, *Physical*
508 *Review C* 95 (6) (2017) 061302. doi:10.1103/PhysRevC.95.061302.
- 509 [14] M. Venhart, J. L. Wood, M. Sedlák, M. Balogh, M. Bírová, A. J.
510 Boston, T. E. Cocolios, L. J. Harkness-Brennan, R.-D. Herzberg, L. Holub,
511 D. T. Joss, D. S. Judson, J. Kliman, J. Klimo, L. Krupa, J. Lušnák,
512 L. Makhathini, V. Matoušek, Š. Motyčák, R. D. Page, A. Patel, K. Petřík,
513 A. V. Podshibyakin, P. M. Prajapati, A. M. Rodin, A. Špaček, R. Urban,
514 C. Unsworth, M. Veselský, New systematic features in the neutron-deficient
515 Au isotopes, *Journal of Physics G: Nuclear and Particle Physics* 44 (7)
516 (2017) 074003. doi:10.1088/1361-6471/aa7297.
- 517 [15] C. Ekström, I. Lindgren, S. Ingelman, M. Olsmats, G. Wannberg, *Nuclear*
518 *spins of 186, 187, 188, 189, 189m Au*, *Physics Letters B* 60 (2) (1976)
519 146–148. doi:10.1016/0370-2693(76)90409-3.
520 URL [http://linkinghub.elsevier.com/retrieve/pii/
521 0370269376904093](http://linkinghub.elsevier.com/retrieve/pii/0370269376904093)
- 522 [16] M. I. Macias-Marques, C. Bourgeois, P. Kilcher, B. Roussière, J. Sauvage,
523 M. C. Abreu, M. G. Porquet, Decays of ^{183}Hg and ^{183}Au , *Nuclear Physics*
524 *A* 427 (2) (1984) 205–223. doi:10.1016/0375-9474(84)90082-4.
- 525 [17] J. Sauvage, C. Bourgeois, P. Kilcher, F. Le Blanc, B. Roussière, M. Macias-
526 Marques, F. Bragança Gil, H. Porquet, H. Dautet, Decays of ^{181}Hg
527 ($T_{1/2}=3.6$ s) and ^{181}Au ($T_{1/2}=11.4$ s), and low-spin states of ^{181}Pt
528 and $^{177,181}\text{Ir}$, *Nuclear Physics A* 540 (1-2) (1992) 83–116. doi:10.1016/
529 *0375-9474(92)90196-q*.

- 530 [18] J. L. Wood, E. F. Zganjar, C. De Coster, K. Heyde, Electric monopole
531 transitions from low energy excitations in nuclei, *Nuclear Physics A* 651 (4)
532 (1999) 323–368. doi:10.1016/S0375-9474(99)00143-8.
- 533 [19] A. N. Andreyev, S. Antalic, D. Ackermann, T. E. Cocolios, V. F. Comas,
534 J. Elseviers, S. Franchoo, S. Heinz, J. A. Heredia, F. P. Heßberger, S. Hof-
535 mann, M. Huyse, J. Khuyagbaatar, I. Kojouharov, B. Kindler, B. Lommel,
536 R. Mann, R. D. Page, S. Rinta-Antila, P. J. Sapple, Š. Šáro, P. V. Dup-
537 pen, M. Venhart, H. V. Watkins, Decay of the 9/2- isomer in ^{181}Tl and
538 mass determination of low-lying states in ^{181}Tl , ^{177}Au , and ^{173}Ir , *Physical*
539 *Review C* 80 (2) (2009) 024302. doi:10.1103/PhysRevC.80.024302.
- 540 [20] M. Venhart, A. N. Andreyev, J. L. Wood, S. Antalic, L. Bianco, P. T.
541 Greenlees, U. Jakobsson, P. Jones, R. Julin, S. Juutinen, S. Ketelhut,
542 M. Leino, M. Nyman, R. D. Page, P. Peura, P. Rahkila, J. Sarén, C. Scholey,
543 J. Sorri, J. Thomson, J. Uusitalo, Shape coexistence in odd-mass Au iso-
544 topes: Determination of the excitation energy of the lowest intruder state
545 in ^{179}Au , *Physics Letters, Section B: Nuclear, Elementary Particle and*
546 *High-Energy Physics* 695 (1-4) (2011) 82–87. doi:10.1016/j.physletb.
547 2010.10.055.
- 548 [21] F. G. Kondev, M. P. Carpenter, R. V. F. Janssens, K. Abu Saleem, I. Ah-
549 mad, H. Amro, J. A. Cizewski, M. Danchev, C. N. Davids, D. J. Hart-
550 ley, A. Heinz, T. L. Khoo, T. Lauritsen, C. J. Lister, W. C. Ma, G. L.
551 Poli, J. Ressler, W. Reviol, L. L. Riedinger, D. Seweryniak, M. B. Smith,
552 I. Wiedenhöver, Identification of excited structures in proton unbound nu-
553 clei $^{173,175,177}\text{Au}$: shape co-existence and intruder bands, *Physics Letters*
554 *B* 512 (3-4) (2001) 268–276. doi:10.1016/S0370-2693(01)00714-6.
- 555 [22] T. Hilberath, S. Becker, G. Bollen, H. J. Kluge, U. Kronert, G. Passler,
556 J. Rikowska, R. Wyss, Ground-state properties of neutron-deficient plat-
557 inum isotopes, *Zeitschrift für Physik A Hadrons and Nuclei* 342 (1) (1992)
558 1–15. doi:10.1007/BF01294481.
- 559 [23] Y. Oktem, D. L. Balabanski, B. Akkus, L. A. Susam, L. Atanasova,
560 C. W. Beausang, R. B. Cakirli, R. F. Casten, M. Danchev, M. Djongolov,
561 E. Ganioglu, K. A. Gladnishki, J. T. Goon, D. J. Hartley, A. A. Hecht,
562 R. Krücken, J. R. Novak, G. Rainovski, L. L. Riedinger, T. Venkova,
563 I. Yigitoglu, N. V. Zamfir, O. Zeidan, Triaxial deformation and nuclear
564 shape transition in ^{192}Au , *Physical Review C* 86 (5) (2012) 054305.
565 doi:10.1103/PhysRevC.86.054305.
- 566 [24] K. S. Toth, X.-J. Xu, C. R. Bingham, J. C. Batchelder, L. F. Conticchio,
567 W. B. Walters, L. T. Brown, C. N. Davids, R. J. Irvine, D. Seweryniak,
568 J. Wauters, E. F. Zganjar, Identification of C 58 (2) (1998) 1310–1313.
569 doi:10.1103/PhysRevC.58.1310.
- 570 [25] A. N. Andreyev, D. Ackermann, F. P. Heßberger, K. Heyde, S. Hof-
571 mann, M. Huyse, D. Karlgren, I. Kojouharov, B. Kindler, B. Lommel,

- 572 G. Münzenberg, R. D. Page, K. Van de Vel, P. Van Duppen, W. B. Wal-
573 ters, R. Wyss, Shape-changing particle decays of ^{185}Bi and structure of
574 the lightest odd-mass Bi isotopes, *Physical Review C* 69 (5) (2004) 054308.
575 [doi:10.1103/PhysRevC.69.054308](https://doi.org/10.1103/PhysRevC.69.054308).
- 576 [26] A. E. Barzakh, A. N. Andreyev, T. E. Cocolios, R. P. de Groote, D. V.
577 Fedorov, V. N. Fedosseev, R. Ferrer, D. A. Fink, L. Ghys, M. Huyse,
578 U. Köster, J. Lane, V. Liberati, K. M. Lynch, B. A. Marsh, P. L. Molka-
579 nov, T. J. Procter, E. Rapisarda, S. Rothe, K. Sandhu, M. D. Seliverstov,
580 A. M. Sjödin, C. Van Beveren, P. Van Duppen, M. Venhart, M. Veselský,
581 Changes in mean-squared charge radii and magnetic moments of $^{179-184}\text{Tl}$
582 measured by in-source laser spectroscopy, *Physical Review C* 95 (1) (2017)
583 014324. [doi:10.1103/PhysRevC.95.014324](https://doi.org/10.1103/PhysRevC.95.014324).
- 584 [27] C. Van Beveren, A. N. Andreyev, A. E. Barzakh, T. E. Cocolios, R. P. D.
585 Groote, D. Fedorov, V. N. Fedosseev, R. Ferrer, L. Ghys, M. Huyse,
586 U. Köster, J. Lane, V. Liberati, K. M. Lynch, B. A. Marsh, P. L. Molka-
587 nov, T. J. Procter, E. Rapisarda, K. Sandhu, M. D. Seliverstov, P. V.
588 Duppen, M. Venhart, M. Veselský, α -decay study of $^{182,184}\text{Tl}$, *Journal of Physics G: Nuclear and Particle Physics* 43 (2) (2016) 025102.
589 [doi:10.1088/0954-3899/43/2/025102](https://doi.org/10.1088/0954-3899/43/2/025102).
- 591 [28] E. Kugler, The ISOLDE facility, *Hyperfine Interactions* 129 (1/4) (2000)
592 23–42. [doi:10.1023/A:1012603025802](https://doi.org/10.1023/A:1012603025802).
- 593 [29] R. Catherall, W. Andreatza, M. Breitenfeldt, A. Dorsival, G. J. Focker,
594 T. P. Gharsa, T. J. Giles, J.-L. Grenard, F. Locci, P. Martins, S. Marzari,
595 J. Schipper, A. Shornikov, T. Stora, The ISOLDE facility, *Journal of*
596 *Physics G: Nuclear and Particle Physics* 44 (9) (2017) 094002. [doi:](https://doi.org/10.1088/1361-6471/aa7eba)
597 [10.1088/1361-6471/aa7eba](https://doi.org/10.1088/1361-6471/aa7eba).
- 598 [30] V. Mishin, V. Fedoseyev, H.-J. Kluge, V. Letokhov, H. Ravn, F. Scheerer,
599 Y. Shirakabe, S. Sundell, O. Tengblad, Chemically selective laser ion-source
600 for the CERN-ISOLDE on-line mass separator facility, *Nuclear Instruments*
601 *and Methods in Physics Research Section B: Beam Interactions with Ma-*
602 *terials and Atoms* 73 (4) (1993) 550–560. [doi:10.1016/0168-583X\(93\)](https://doi.org/10.1016/0168-583X(93)95839-W)
603 [95839-W](https://doi.org/10.1016/0168-583X(93)95839-W).
- 604 [31] V. Fedosseev, K. Chrysalidis, T. D. Goodacre, B. Marsh, S. Rothe, C. Seif-
605 fert, K. Wendt, Ion beam production and study of radioactive isotopes with
606 the laser ion source at ISOLDE, *Journal of Physics G: Nuclear and Particle*
607 *Physics* 44 (8) (2017) 084006. [doi:10.1088/1361-6471/aa78e0](https://doi.org/10.1088/1361-6471/aa78e0).
- 608 [32] R. N. Wolf, F. Wienholtz, D. Atanasov, D. Beck, K. Blaum, C. Borgmann,
609 F. Herfurth, M. Kowalska, S. Kreim, Y. A. Litvinov, D. Lunney, V. Manea,
610 D. Neidherr, M. Rosenbusch, L. Schweikhard, J. Stanja, K. Zuber,
611 ISOLTRAP’s multi-reflection time-of-flight mass separator/spectrometer,
612 *International Journal of Mass Spectrometry* 349-350 (1) (2013) 123–133.
613 [doi:10.1016/j.ijms.2013.03.020](https://doi.org/10.1016/j.ijms.2013.03.020).

- 614 [33] H. De Witte, A. N. Andreyev, N. Barre, M. Bender, T. E. Cocolios,
615 S. Dean, D. Fedorov, V. N. Fedoseyev, L. M. Fraile, S. Franchoo, V. Helle-
616 mans, P. H. Heenen, K. Heyde, G. Huber, M. Huyse, H. Jeppessen,
617 U. Köster, P. Kunz, S. R. Leshner, B. A. Marsh, I. Mukha, B. Roussi re,
618 J. Sauvage, M. Seliverstov, I. Stefanescu, E. Tengborn, K. Van De Vel,
619 J. Van De Walle, P. Van Duppen, Y. Volkov, Nuclear charge radii of
620 neutron-deficient lead isotopes beyond N=104 midshell investigated by in-
621 source laser spectroscopy, *Physical Review Letters* 98 (11) (2007) 16–19.
622 [doi:10.1103/PhysRevLett.98.112502](https://doi.org/10.1103/PhysRevLett.98.112502).
- 623 [34] A. N. Andreyev, J. Elseviers, M. Huyse, P. Van Duppen, S. Antalic,
624 A. Barzakh, N. Bree, T. E. Cocolios, V. F. Comas, J. Diriken, D. Fedorov,
625 V. Fedosseev, S. Franchoo, J. A. Heredia, O. Ivanov, U. K ster, B. A.
626 Marsh, K. Nishio, R. D. Page, N. Patronis, M. Seliverstov, I. Tsekhanovich,
627 P. Van Den Bergh, J. Van De Walle, M. Venhart, S. Vermote, M. Veselsky,
628 C. Wagemans, T. Ichikawa, A. Iwamoto, P. M ller, A. J. Sierk, Others,
629 New Type of Asymmetric Fission in Proton-Rich Nuclei, *Physical Review*
630 *Letters* 105 (25) (2010) 1–5. [doi:10.1103/PhysRevLett.105.252502](https://doi.org/10.1103/PhysRevLett.105.252502).
- 631 [35] J. G. Cubiss, A. E. Barzakh, M. D. Seliverstov, A. N. Andreyev, B. An-
632 del, S. Antalic, P. Ascher, D. Atanasov, D. Beck, J. Biero n, K. Blaum,
633 C. Borgmann, M. Breitenfeldt, L. Capponi, T. E. Cocolios, T. Day
634 Goodacre, X. Derkx, H. De Witte, J. Elseviers, D. V. Fedorov, V. N. Fe-
635 dosseev, S. Fritzsche, L. P. Gaffney, S. George, L. Ghys, F. P. He berger,
636 M. Huyse, N. Imai, Z. Kalaninov , D. Kisler, U. K ster, M. Kowalska,
637 S. Kreim, J. F. W. Lane, V. Liberati, D. Lunney, K. M. Lynch, V. Manea,
638 B. A. Marsh, S. Mitsuoka, P. L. Molkanov, Y. Nagame, D. Neidherr,
639 K. Nishio, S. Ota, D. Pauwels, L. Popescu, D. Radulov, E. Rapisarda, J. P.
640 Revill, M. Rosenbusch, R. E. Rossel, S. Rothe, K. Sandhu, L. Schweikhard,
641 S. Sels, V. L. Truesdale, C. Van Beveren, P. Van den Bergh, Y. Wak-
642 abayashi, P. Van Duppen, K. D. A. Wendt, F. Wienholtz, B. W. Whit-
643 more, G. L. Wilson, R. N. Wolf, K. Zuber, Charge radii and electromag-
644 netic moments of 195-211At, *Physical Review C* 97 (5) (2018) 054327.
645 [doi:10.1103/PhysRevC.97.054327](https://doi.org/10.1103/PhysRevC.97.054327).
- 646 [36] M. D. Seliverstov, T. E. Cocolios, W. Dexters, A. N. Andreyev, S. Antalic,
647 A. E. Barzakh, B. Bastin, J. B scher, I. G. Darby, D. V. Fedorov, V. N.
648 Fedosseev, K. T. Flanagan, S. Franchoo, G. Huber, M. Huyse, M. Keupers,
649 U. K ster, Y. Kudryavtsev, B. A. Marsh, P. L. Molkanov, R. D. Page, A. M.
650 Sj din, I. Stefan, P. Van Duppen, M. Venhart, S. G. Zemlyanoy, Electro-
651 magnetic moments of odd-A 193-203,211Po isotopes, *Physical Review C*
652 89 (3) (2014) 034323. [doi:10.1103/PhysRevC.89.034323](https://doi.org/10.1103/PhysRevC.89.034323).
- 653 [37] B. A. Marsh, V. N. Fedosseev, P. Kosuri, Development of a RILIS ionisation
654 scheme for gold at ISOLDE, CERN, *Hyperfine Interactions* 171 (1-3) (2006)
655 109–116. [doi:10.1007/s10751-006-9498-8](https://doi.org/10.1007/s10751-006-9498-8).

- 656 [38] NNDC, Evaluated nuclear structure data file, Evaluated Nuclear Structure
657 Data File.
- 658 [39] V. A. Bolshakov, A. G. Dernjatin, K. A. Mezilev, Y. N. Novikov, A. V.
659 Popov, Y. Y. Sergeev, V. I. Tikhonov, V. A. Sergienko, G. V. Veselov, in:
660 Nuclei Far From Stability/Atomic Masses and Fundamental Constants 1992,
661 6th International Conference on Nuclei Far from Stability (NFFS 6) Jointly
662 with 9th International Conference on Atomic Masses and Fundamental
663 Constants (AMCO 9) Bernkastel-Kues, Germany, July 19-25, 1992, 1992.
- 664 [40] K. S. Toth, J. C. Batchelder, C. R. Bingham, L. F. Conticchio, W. B.
665 Walters, C. N. Davids, D. J. Henderson, R. Herman, H. Penttilä, J. D.
666 Richards, A. H. Wuosmaa, B. E. Zimmerman, α -decay properties of ^{181}Pb ,
667 Physical Review C 53 (5) (1996) 2513–2515. doi:10.1103/PhysRevC.53.
668 2513.
- 669 [41] F. James, M. Roos, Minuit - a system for function minimization and anal-
670 ysis of the parameter errors and correlations, Computer Physics Commu-
671 nications 10 (6) (1975) 343–367. doi:10.1016/0010-4655(75)90039-9.
- 672 [42] M. J. Oreglia, A study of the reactions $\psi' \rightarrow j \gamma \gamma \psi$,
673 Ph.D. Thesis, SLAC-R-236.
- 674 [43] J. E. Gaiser, Charmonium spectroscopy from radiative decays of the j/ψ
675 and ψ' , Ph.D. Thesis, SLAC-R-255.
- 676 [44] T. Skwarnicki, A study of the radiative cascade transitions between the
677 ψ' and ψ resonances, Ph.D Thesis, DESY F31-86-02.
- 678 [45] J. O. Rasmussen, Alpha-Decay Barrier Penetrabilities with an Exponential
679 Nuclear Potential: Even-Even Nuclei, Physical Review 113 (6) (1959) 1593–
680 1598. doi:10.1103/PhysRev.113.1593.
- 681 [46] R. D. Harding, et al., unpublished.
- 682 [47] G. D. Dracoulis, B. Fabricius, T. Kibedi, A. M. Baxter, A. P. Byrne, K. P.
683 Lieb, A. E. Stuchbery, Spectroscopy of ^{175}Ir and ^{177}Ir and deformation
684 effects in odd iridium nuclei, Nuclear Physics A 534 (1) (1991) 173–203.
685 doi:10.1016/0375-9474(91)90562-K.
- 686 [48] B. Cederwall, B. Fant, R. Wyss, A. Johnson, J. Nyberg, J. Simpson, A. M.
687 Bruce, J. N. Mo, High-spin states of ^{175}Ir : Quasiproton-induced shapes
688 and extreme, Physical Review C 43 (5) (1991) R2031–R2034. doi:10.
689 1103/PhysRevC.43.R2031.
- 690 [49] S. D. Gillespie, et al., unpublished.
- 691 [50] A. Bohr, V. F. Weisskopf, The Influence of Nuclear Structure on the Hy-
692 perfine Structure of Heavy Elements, Physical Review 77 (1) (1950) 94–98.
693 doi:10.1103/PhysRev.77.94.

- 694 [51] P. Moskowitz, M. Lombardi, Distribution of nuclear magnetization in mer-
695 cury isotopes, *Physics Letters B* 46 (3) (1973) 334–336. doi:10.1016/
696 0370-2693(73)90132-9.
- 697 [52] N. Frömmgen, D. L. Balabanski, M. L. Bissell, J. Bieroń, K. Blaum,
698 B. Cheal, K. Flanagan, S. Fritzsche, C. Geppert, M. Hammen, M. Kowal-
699 ska, K. Kreim, A. Krieger, R. Neugart, G. Neyens, M. M. Rajabali,
700 W. Nörtershäuser, J. Papuga, D. T. Yordanov, *Collinear laser spectroscopy*
701 *of atomic cadmium*, *The European Physical Journal D* 69 (6) (2015) 164.
702 doi:10.1140/epjd/e2015-60219-0.
703 URL <http://link.springer.com/10.1140/epjd/e2015-60219-0>
- 704 [53] J. R. Persson, Table of hyperfine anomaly in atomic systems, *Atomic Data*
705 *and Nuclear Data Tables* 99 (1) (2013) 62–68. doi:10.1016/j.adt.2012.
706 04.002.
- 707 [54] G. L. Poli, C. N. Davids, P. J. Woods, D. Seweryniak, J. C. Batchelder,
708 L. T. Brown, C. R. Bingham, M. P. Carpenter, L. F. Conticchio, T. Davin-
709 son, J. DeBoer, S. Hamada, D. J. Henderson, R. J. Irvine, R. V. F. Janssens,
710 H. J. Maier, L. Muller, F. Soramel, K. S. Toth, W. B. Walters, J. Wauters,
711 Proton and alpha radioactivity below the Z=82 shell closure, *Physical Re-
712 view C* 59 (6) (1999) R2979–R2983. doi:10.1103/PhysRevC.59.R2979.
- 713 [55] A. Thorntwaite, D. O’Donnell, R. D. Page, D. T. Joss, C. Scholey,
714 L. Bianco, L. Capponi, R. J. Carroll, I. G. Darby, L. Donosa, M. C. Drum-
715 mond, F. Ertuğral, T. Grahn, P. T. Greenlees, K. Hauschild, A. Herzan,
716 U. Jakobsson, P. Jones, R. Julin, S. Juutinen, S. Ketelhut, M. Labiche,
717 M. Leino, A. Lopez-Martens, K. Mullholland, P. Nieminen, P. Peura,
718 P. Rahkila, S. Rinta-Antila, P. Ruotsalainen, M. Sandzelius, J. Sarén,
719 B. Saygi, J. Simpson, J. Sorri, J. Uusitalo, Characterizing the atomic mass
720 surface beyond the proton drip line via α -decay measurements of the $\pi_{S1/2}$
721 ground state of ^{165}Re and the $\pi_{h_{11/2}}$ isomer in ^{161}Ta , *Physical Review C*
722 86 (6) (2012) 064315. doi:10.1103/PhysRevC.86.064315.
- 723 [56] A. N. Andreyev, V. Liberati, S. Antalic, D. Ackermann, A. Barzakh,
724 N. Bree, T. E. Cocolios, J. Diriken, J. Elseviers, D. Fedorov, V. N.
725 Fedosseev, D. Fink, S. Franchoo, S. Heinz, F. P. Heßberger, S. Hof-
726 mann, M. Huyse, O. Ivanov, J. Khuyagbaatar, B. Kindler, U. Köster,
727 J. F. W. Lane, B. Lommel, R. Mann, B. Marsh, P. Molkanov, K. Nishio,
728 R. D. Page, N. Patronis, D. Pauwels, D. Radulov, Š. Šáro, M. Seliver-
729 stov, M. Sjödin, I. Tsekhanovich, P. Van Den Bergh, P. Van Duppen,
730 M. Venhart, M. Veselský, α -decay spectroscopy of the chain $^{179}\text{Tl}^g \rightarrow ^{175}\text{Au}^g$
731 $\rightarrow ^{171}\text{Ir}^g \rightarrow ^{167}\text{Re}^m$, *Physical Review C - Nuclear Physics* 87 (5) (2013) 1–8.
732 doi:10.1103/PhysRevC.87.054311.
- 733 [57] H. Kettunen, T. Enqvist, T. Grahn, P. T. Greenlees, P. Jones, R. Julin,
734 S. Juutinen, A. Keenan, P. Kuusiniemi, M. Leino, A. P. Leppänen, P. Niemi-
735 nen, J. Pakarinen, P. Rahkila, J. Uusitalo, Alpha-decay studies of the new

- 736 isotopes ^{191}At and ^{193}At , *European Physical Journal A* 17 (4) (2003) 537–
737 558. doi:10.1140/epja/i2002-10162-1.
- 738 [58] H. Kettunen, T. Enqvist, M. Leino, K. Eskola, P. T. Greenlees, K. Helariutta,
739 P. Jones, R. Julin, S. Juutinen, H. Kankaanpää, H. Koivisto, P. Kuusiniemi,
740 M. Muikku, P. Nieminen, P. Rahkila, J. Uusitalo, Investigations
741 into the alpha-decay of ^{195}At , *The European Physical Journal A* 16 (4)
742 (2003) 457–467. doi:10.1140/epja/i2002-10130-9.
- 743 [59] J. Uusitalo, M. Leino, T. Enqvist, K. Eskola, T. Grahn, P. T. Greenlees,
744 P. Jones, R. Julin, S. Juutinen, A. Keenan, H. Kettunen, H. Koivisto,
745 P. Kuusiniemi, A.-P. Leppänen, P. Nieminen, J. Pakarinen, P. Rahkila,
746 C. Scholey, α decay studies of very neutron-deficient francium and radium
747 isotopes, *Physical Review C* 71 (2) (2005) 024306. doi:10.1103/
748 PhysRevC.71.024306.
- 749 [60] M. B. Smith, R. Chapman, J. F. C. Cocks, O. Dorvaux, K. Helariutta, P. M.
750 Jones, R. Julin, S. Juutinen, H. Kankaanpää, H. Kettunen, P. Kuusiniemi,
751 Y. Le Coz, M. Leino, D. J. Middleton, M. Muikku, P. Nieminen, P. Rahkila,
752 A. Savelius, K.-M. Spohr, First observation of excited states in ^{197}At : the
753 onset of deformation in neutron-deficient astatine nuclei, *European Physical*
754 *Journal A* 47 (1999) 43–47. doi:10.1007/s100500050254.
- 755 [61] U. Jakobsson, S. Juutinen, J. Uusitalo, M. Leino, K. Auranen, T. Enqvist,
756 P. T. Greenlees, K. Hauschild, P. Jones, R. Julin, S. Ketelhut, P. Kuusiniemi,
757 M. Nyman, P. Peura, P. Rahkila, P. Ruotsalainen, J. Sarén,
758 C. Scholey, J. Sorri, Spectroscopy of the proton drip-line nucleus ^{203}Fr ,
759 *Physical Review C* 87 (5) (2013) 1–9. doi:10.1103/PhysRevC.87.054320.
- 760 [62] A. N. Andreyev, S. Antalic, D. Ackermann, S. Franchoo, F. P. Heßberger,
761 S. Hofmann, M. Huyse, I. Kojouharov, B. Kindler, P. Kuusiniemi, S. R.
762 Leshner, B. Lommel, R. Mann, G. Münzenberg, K. Nishio, R. D. Page, J. J.
763 Ressler, B. Streicher, S. Saro, B. Sulignano, P. V. Duppen, D. Wiseman,
764 R. Wyss, α -decay of the new isotope ^{187}Po : Probing prolate structures
765 beyond the neutron mid-shell at $n = 104$, *Physical Review C* 73 (4) (2006)
766 044324. doi:10.1103/PhysRevC.73.044324.
- 767 [63] E. Coenen, K. Deneffe, M. Huyse, P. V. Duppen, J. L. Wood, α Decay
768 of Neutron-Deficient Odd Bi Nuclei: Shell-Model Intruder States in Tl
769 and Bi Isotopes, *Physical Review Letters* 54 (16) (1985) 1783–1786. doi:
770 10.1103/PhysRevLett.54.1783.
- 771 [64] C. Scholey, M. Sandzelius, S. Eeckhaudt, T. Grahn, P. T. Greenlees,
772 P. Jones, R. Julin, S. Juutinen, M. Leino, A.-P. Leppänen, P. Nieminen,
773 M. Nyman, J. Perkowski, J. Pakarinen, P. Rahkila, P. M. Rahkila, J. Uusi-
774 talo, K. V. de Vel, B. Cederwall, B. Hadinia, K. Lagergren, D. T. Joss, D. E.
775 Appelbe, C. J. Barton, J. Simpson, D. D. Warner, I. G. Darby, R. D. Page,
776 E. S. Paul, D. Wiseman, In-beam and decay spectroscopy of very neutron

- 777 deficient iridium nuclei, *Journal of Physics G: Nuclear and Particle Physics*
778 31 (10) (2005) S1719–S1722. doi:[10.1088/0954-3899/31/10/061](https://doi.org/10.1088/0954-3899/31/10/061).
- 779 [65] M. W. Rowe, J. C. Batchelder, T. N. Ginter, K. E. Gregorich, F. Q. Guo,
780 F. P. Hessberger, V. Ninov, J. Powell, K. S. Toth, X. J. Xu, J. Cerny,
781 Decay of ^{178}Tl , *Physical Review C* 65 (5) (2002) 054310. doi:[10.1103/
782 PhysRevC.65.054310](https://doi.org/10.1103/PhysRevC.65.054310).
- 783 [66] A. N. Andreyev, M. Huyse, P. Van Duppen, C. Qi, R. J. Liotta, S. Antalic,
784 D. Ackermann, S. Franchoo, F. P. Heßberger, S. Hofmann, I. Kojouharov,
785 B. Kindler, P. Kuusiniemi, S. R. Leshner, B. Lommel, R. Mann, K. Nishio,
786 R. D. Page, B. Streicher, Š. Šáro, B. Sulignano, D. Wiseman, R. A. Wyss,
787 Signatures of the $Z=82$ Shell Closure in α -Decay Process, *Physical Review*
788 *Letters* 110 (24) (2013) 242502. doi:[10.1103/PhysRevLett.110.242502](https://doi.org/10.1103/PhysRevLett.110.242502).
- 789 [67] C. Qi, A. N. Andreyev, M. Huyse, R. J. Liotta, P. Van Duppen, R. Wyss,
790 On the validity of the Geiger–Nuttall alpha-decay law and its microscopic
791 basis, *Physics Letters B* 734 (2014) 203–206. doi:[10.1016/j.physletb.
792 2014.05.066](https://doi.org/10.1016/j.physletb.2014.05.066).
- 793 [68] Y. A. Akovali, Review of alpha-decay data from doubly-even nuclei, *Nu-*
794 *clear Data Sheets* 84 (1) (1998) 1 – 114. doi:[https://doi.org/10.1006/
795 ndsh.1998.0009](https://doi.org/10.1006/ndsh.1998.0009).
- 796 [69] F. G. Kondev, R. V. F. Janssens, M. P. Carpenter, K. Abu Saleem, I. Ah-
797 mad, M. Alcorta, H. Amro, P. Bhattacharyya, L. T. Brown, J. Caggiano,
798 C. N. Davids, S. M. Fischer, A. Heinz, B. Herskind, R. A. Kaye, T. L. Khoo,
799 T. Lauritsen, C. J. Lister, W. C. Ma, R. Nouicer, J. Ressler, W. Reviol,
800 L. L. Riedinger, D. G. Sarantites, D. Seweryniak, S. Siem, A. A. Sonzogni,
801 J. Uusitalo, P. G. Varmette, I. Wiedenhöver, Interplay between octupole
802 and quasiparticle excitations in ^{178}Hg and ^{180}Hg , *Physical Review C* 62 (4)
803 (2000) 044305. doi:[10.1103/PhysRevC.62.044305](https://doi.org/10.1103/PhysRevC.62.044305).
- 804 [70] S.-C. Wu, H. Niu, Nuclear data sheets for $a = 180$, *Nuclear Data Sheets*
805 100 (4) (2003) 483 – 705. doi:[10.1006/ndsh.2003.0018](https://doi.org/10.1006/ndsh.2003.0018).
- 806 [71] P. Möller, A. Sierk, R. Bengtsson, H. Sagawa, T. Ichikawa, Nuclear shape
807 isomers, *Atomic Data and Nuclear Data Tables* 98 (2) (2012) 149–300.
808 doi:[10.1016/j.adt.2010.09.002](https://doi.org/10.1016/j.adt.2010.09.002).
- 809 [72] N. J. Stone, Table of nuclear magnetic dipole and electric quadrupole
810 moments, *Atomic Data and Nuclear Data Tables* 90 (1) (2005) 75–176.
811 doi:[10.1016/j.adt.2005.04.001](https://doi.org/10.1016/j.adt.2005.04.001).
- 812 [73] J. A. Bounds, C. R. Bingham, H. K. Carter, G. A. Leander, R. L. Mleko-
813 daj, E. H. Spejewski, W. M. Fairbank, Nuclear structure of light thallium
814 isotopes as deduced from laser spectroscopy on a fast atom beam, *Physical*
815 *Review C* 36 (6) (1987) 2560–2568. doi:[10.1103/PhysRevC.36.2560](https://doi.org/10.1103/PhysRevC.36.2560).

- 816 [74] R. Menges, U. Dinger, N. Boos, G. Huber, S. Schröder, S. Dutta, R. Kirchner,
817 O. Klepper, T. U. Kühl, D. Marx, G. D. Sprouse, Nuclear moments
818 and the change in the mean square charge radius of neutron deficient thal-
819 lium isotopes, *Zeitschrift für Physik A Hadrons and Nuclei* 341 (4) (1992)
820 475–479. [doi:10.1007/BF01301392](https://doi.org/10.1007/BF01301392).
- 821 [75] H. A. Schuessler, E. C. Benck, F. Buchinger, H. Iimura, Y. F. Li, C. Bingham,
822 H. K. Carter, Nuclear moments of the neutron-deficient thallium
823 isotopes, *Hyperfine Interactions* 74 (1-4) (1992) 13–21. [doi:10.1007/
824 BF02398612](https://doi.org/10.1007/BF02398612).
- 825 [76] A. E. Barzakh, L. K. Batist, D. V. Fedorov, V. S. Ivanov, K. A. Mezilev,
826 P. L. Molkanov, F. V. Moroz, S. Y. Orlov, V. N. Panteleev, Y. M. Volkov,
827 Changes in the mean-square charge radii and magnetic moments of neutron-
828 deficient Tl isotopes, *Physical Review C* 88 (2) (2013) 1–10. [doi:10.1103/
829 PhysRevC.88.024315](https://doi.org/10.1103/PhysRevC.88.024315).
- 830 [77] A. E. Barzakh, D. V. Fedorov, V. S. Ivanov, P. L. Molkanov, F. V. Mo-
831 roz, S. Y. Orlov, V. N. Panteleev, M. D. Seliverstov, Y. M. Volkov, Laser
832 spectroscopy studies of intruder states in $^{193,195,197}\text{Bi}$, *Physical Review C*
833 94 (2) (2016) 024334. [doi:10.1103/PhysRevC.94.024334](https://doi.org/10.1103/PhysRevC.94.024334).
- 834 [78] G. Neyens, Nuclear magnetic and quadrupole moments for nuclear structure
835 research on exotic nuclei, *Reports on Progress in Physics* 66 (4) (2003)
836 633–689. [doi:10.1088/0034-4885/66/4/205](https://doi.org/10.1088/0034-4885/66/4/205).
- 837 [79] C. N. Davids, P. J. Woods, J. C. Batchelder, C. R. Bingham, D. J. Blumenthal,
838 L. T. Brown, B. C. Busse, L. F. Conticchio, T. Davinson, S. J. Freeman,
839 D. J. Henderson, R. J. Irvine, R. D. Page, H. T. Penttilä, D. Seweryniak,
840 K. S. Toth, W. B. Walters, B. E. Zimmerman, New proton radioactivities
841 $^{165,166,167}\text{Ir}$ and ^{171}Au , *Physical Review C* 55 (5) (1997) 2255–2266.
842 [doi:10.1103/PhysRevC.55.2255](https://doi.org/10.1103/PhysRevC.55.2255).
- 843 [80] H. Kettunen, T. Enqvist, T. Grahn, P. T. Greenlees, P. Jones, R. Julin,
844 S. Juutinen, A. Keenan, P. Kuusiniemi, M. Leino, A. P. Leppänen, P. Nieminen,
845 J. Pakarinen, P. Rahkila, J. Uusitalo, Decay studies of $^{170,171}\text{Au}$,
846 $^{171-173}\text{Hg}$, and ^{176}Tl , *Physical Review C - Nuclear Physics* 69 (5) (2004)
847 054323–1. [doi:10.1103/PhysRevC.69.054323](https://doi.org/10.1103/PhysRevC.69.054323).